Observation of anticorrelation between scintillation and ionization for MeV gamma rays in liquid xenon

E. Aprile, K. L. Giboni, P. Majewski,* K. Ni,† and M. Yamashita
Physics Department and Columbia Astrophysics Laboratory, Columbia University, New York, New York 10027, USA
(Received 27 March 2007; published 25 July 2007)

A strong anticorrelation between ionization and scintillation signals produced by MeV γ rays in liquid xenon has been measured and used to improve the energy resolution by combining the two signals. The improvement is explained by reduced electron-ion recombination fluctuations of the combined signal compared to fluctuations of the individual signals. Simultaneous measurements of ionization and scintillation signals were carried out with ^{137}Cs, ^{22}Na, and ^{60}Co γ rays, as a function of electric field in the liquid. A resolution of 1.7% (σ) at 662 keV was measured at 1 kV/cm, significantly better than the resolution from either scintillation or ionization alone. A detailed analysis indicates that further improvement to less than 1% (σ) is possible with higher light collection efficiency and lower electronic noise.

DOI: 10.1103/PhysRevB.76.014115 PACS number(s): 78.70.−g, 29.30.Kv, 34.80.Gs, 29.40.Mc

I. INTRODUCTION

Liquid xenon (LXe) is an excellent medium for radiation detection, with high stopping power, good ionization, and scintillation yields. Currently, liquid xenon detectors are being developed for several fundamental particle physics experiments, from neutrinoless double beta decay[1] and dark matter weakly interactive massive particle detection,[2–5] to spectroscopy and imaging of gamma rays in physics, astrophysics, and nuclear medicine.[6–9] A more precise energy measurement than currently demonstrated with liquid xenon ionization and scintillation detectors would largely benefit all these experiments. The best experimental energy resolution is not only orders of magnitude worse than that expected from the Fano factor[10] but even worse than that predicted by the Poisson statistics, based on the measured W value of 15.6 eV.[11] The reason for the discrepancy is yet to be fully understood, but fluctuations in electron-ion pair recombination rate are known to play a dominant role.

Both electron-ion pairs and excitons are produced by the passage of an ionizing particle in liquid xenon. In the presence of an electric field, some of the electron-ion pairs are separated before recombination, providing the charge signal as electrons drift freely in the field. Recombination of the remaining electron-ion pairs leads to excited xenon molecules, Xe_2^*. Excitons that are directly produced by the incident particle also become Xe_2^* molecules. Deexcitation of these molecules to the ground state, $Xe_2^* \rightarrow 2Xe + h\nu$, produces scintillation photons with a wavelength of 178 nm.[12] The ionization and scintillation signals in liquid xenon are thus complementary and anticorrelated as the suppression of recombination by the external field results in more free electrons and less scintillation photons.

This anticorrelation was first observed by Kubota *et al.*[13] Large fluctuations in the number of collected electrons due to their reduction by recombination lead to poor energy resolution of the ionization signal. A way to increase the ionization signal and thus the energy resolution via the photoionization effect in LXe doped with triemethylamine yielded good results, but only at low electric fields.[14] Another way to improve the energy resolution is to reduce recombination fluctuations by combining ionization and scintillation signals. Since recombination also produces scintillation photons, fluctuations of the combined signal should be reduced. This was originally suggested by Ypsilantis *et al.* many years ago.[15] The simultaneous detection of scintillation and ionization in LXe has, however, been hard to realize because of the difficulty to efficiently detect VUV light under the constraints of efficient charge collection.

In the Liquid Xenon Gamma-Ray Imaging Telescope (LXeGRIT),[7] developed for Compton imaging of cosmic γ rays, both ionization and scintillation are detected, but the fast vuv scintillation signal merely provided the event trigger. The ionization signal provided the energy measurement, with a resolution of 4.2% (σ) at 1 MeV. The fair resolution has been a major limitation of the LXe time projection chamber (TPC) technology for astrophysics. In recent years, the development of vuv-sensitive photomultiplier tubes (PMTs), capable of operating directly in the cryogenic liquid, has resulted in significant improvement of the Xe scintillation light collection efficiency with good uniformity across the liquid volume. A light readout based on these novel PMTs, coupled with a lower-noise charge readout, was proposed to measure both signals event by event and thus to improve the energy resolution and the Compton imaging of the LXeGRIT telescope.[16] The work presented here was carried out with two of the first PMTs developed for operation in LXe and is our first attempt in this direction. Further optimization of these vuv PMTs has continued, driven largely by our XENON dark matter detector development.[2,17] These improved PMTs, along with other vuv sensor technologies such as large area avalanche photodiodes and Si photomultipliers, which we are also testing for LXe scintillation detection,[18,19] promise further energy resolution improvement.

II. EXPERIMENTAL SETUP AND SIGNALS

The detector used for this study is a gridded ionization chamber with two vuv sensitive PMTs (2-in.-diameter Hamamatsu R9288) viewing the sensitive liquid xenon volume from the anode, and cathode sides. The two PMTs, and the transparent meshes serving as anode, cathode and shield-

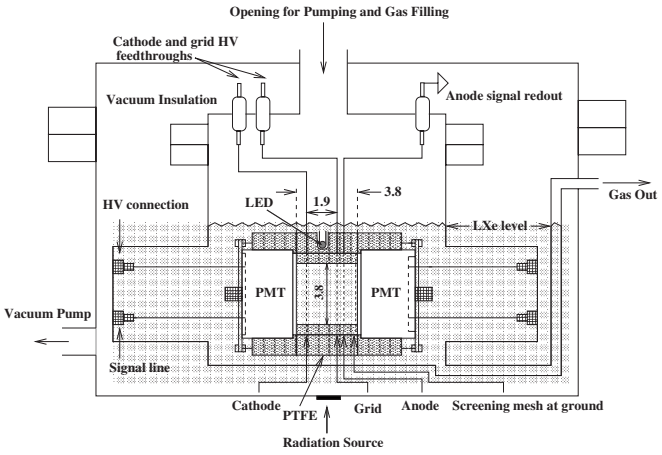

FIG. 1. The detector schematics (see text for details).

ing grid, are mounted in a structure made of Teflon for its vuv reflectivity[20] (Fig. 1). The drift gap, between cathode and grid, is 1.9 cm, while the distance between grid and anode is 3 mm. Separate high voltage is supplied to the cathode and the grid, keeping a ratio between the field in the drift gap and the field in the collection gap such as to maximize electron transmission through the grid. The electrons collected on the anode are detected by a charge-sensitive amplifier (ClearPulse model 580). The charge signal is subsequently digitized with 10 bit resolution and a sampling time of 200 ns (LeCroy model 2262). The scintillation signal from each of the two PMTs is recorded with a digital oscilloscope (LeCroy model LT374) with 1 ns sampling time. The time difference between the scintillation and ionization signals is the electron drift time which gives the event depth-of-interaction information. The coincidence of the two PMT signals is used as event trigger. Figure 2 shows the scintillation and ionization wave forms recorded at 1 kV/cm for a 662 keV γ-ray event from ^{137}Cs. The number of photoelectrons N_{pe} detected by the PMTs is calculated based on the gain calibration with a light emitting diode. The charge wave

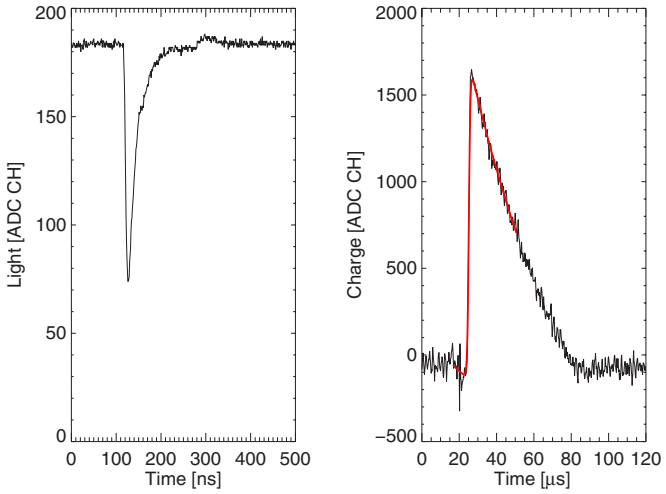

FIG. 2. (Color online) Wave forms of scintillation signal (left, sum of two PMTs) and ionization signal (right) of a 662 keV γ-ray event from ^{137}Cs at 1 kV/cm drift field.

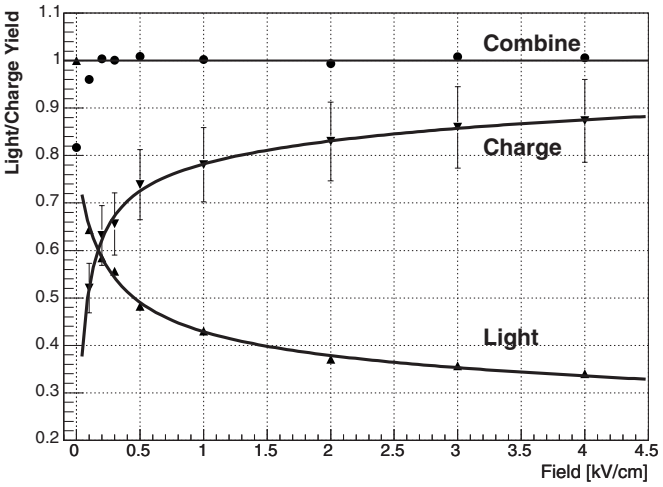

FIG. 3. Light and charge yields as a function of drift field for 662 keV γ rays from ^{137}Cs. The uncertainty for charge measurement is due to the uncertainty in preamplifier calibration. The light yield is relative to that at zero field, for which the systematic uncertainty is negligible.

form is well described by the Fermi-Dirac threshold function in Eq. (1), as shown in Ref. 21. The pulse height A, drift time t_d, rise time t_r, and fall time t_f are determined from fitting Eq. (1) to the charge wave form. A known test pulse is used to calibrate the charge readout system, and the number of collected electrons N_e is calculated from the pulse height of the charge wave form.

$$Q(t) = A\frac{e^{-(t-t_d)/t_r}}{1+e^{-(t-t_d)/t_f}}. \quad (1)$$

The Teflon structure holding the PMTs and the meshes is mounted in a stainless steel vessel filled with liquid xenon at about −95 °C during the experiment. A vacuum cryostat surrounds the vessel for thermal insulation. The xenon gas filling and purification system, as well as the "cold finger" system used for this setup, is described in a previous publication.[21] The setup was modified for these measurements by adding a gas recirculation system[17] in order to purify the xenon continuously until sufficient charge collection is reached.

III. RESULTS AND DISCUSSION

A. Field dependence of scintillation and ionization

Figure 3 shows our measurement of the field dependence up to 4 kV/cm of the light and charge yields for 662 keV γ rays from ^{137}Cs. With increasing drift field, the charge yield increases, while the light yield decreases. This behavior has been known for a long time, and was originally reported in Ref. 13.

A parametrization of the field dependence of the light yield, $S(E)/S_0$, was proposed by Doke *et al.*,[22] introducing the model of escaping electrons to explain the scintillation light reduction at low linear energy transfer. In this parametrization, expressed by Eq. (2), the light yield $S(E)$ at drift

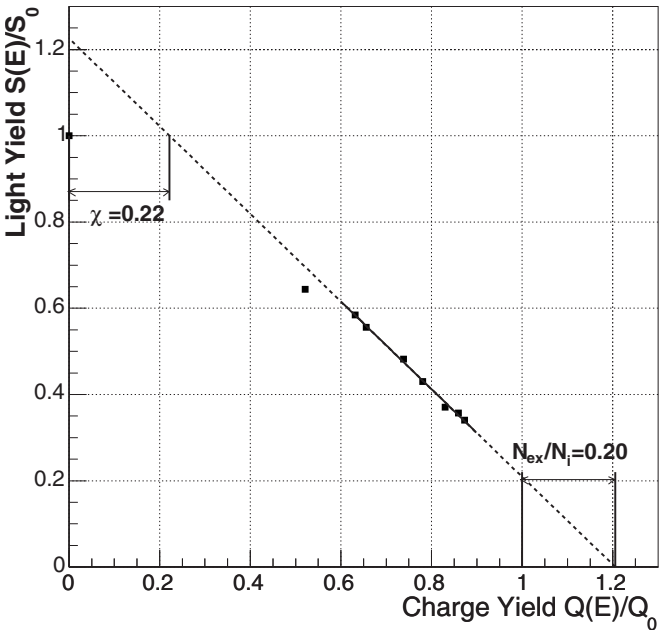

FIG. 4. Correlation between light yields and charge yield for 662 keV γ rays.

field E, normalized by the light yield at zero field, S_0, depends on the charge yield $Q(E)$ normalized to the charge at infinite field, Q_0, and on the ratio N_{ex}/N_i of the number of excitons and ion pairs produced by a γ ray. χ is the fraction of escaping electrons, i.e., the fraction of N_i electrons which do not recombine with positive ions for an extended time (greater than millisecond) even at zero field, when the probability of recombination is highest.

$$\frac{S(E)}{S_0} = \frac{1 + N_{ex}/N_i - Q(E)/Q_0}{1 + N_{ex}/N_i - \chi}. \tag{2}$$

N_{ex}/N_i and χ can be determined from a fit of Eq. (2) to the charge and light yield data knowing Q_0, which is given by E_γ/W, where E_γ is the γ-ray deposited energy and $W=15.6$ eV (Ref. 11) is the average energy required to produce an electron-ion pair in liquid xenon.

Figure 4 shows the result of such a fit to our 662 keV data, which gives $N_{ex}/N_i=0.20\pm0.13$ and $\chi=0.22\pm0.02$. The errors are from the uncertainty on charge collection only. A ratio of 0.06 for N_{ex}/N_i was originally estimated from the optical approximation, using the absorption spectrum of solid rare gases.[23] In Ref. 22. $N_{ex}/N_i=0.20$ and $\chi=0.43$ as estimated from 1 MeV conversion electron data in LXe. This N_{ex}/N_i value is consistent with that obtained from our data. The difference in χ might be due to the limited range of electric fields used in our study.

The charge and light signals can be combined by the following equation:

$$C(E) = a\frac{Q(E)}{Q_0} + b\frac{S(E)}{S_0}, \tag{3}$$

with $a=1/[1+(N_{ex}/N_i)]$ and $b=1-a\chi$, which gives a constant $C(E)=1$, regardless of applied field. The proportion of charge and light is different at different fields but their sum is constant, as verified by our data in Fig. 3. Note that at very low fields, Eqs. (2) and (3) are not valid as escaping electrons are not fully collected.

B. Combined energy from scintillation and ionization

The observed field dependent anticorrelation between charge and light signals and its linear relationship offers a way to improve the energy resolution by combining the two signals with proper coefficients. This was first shown in a measurement of energy loss of relativistic La ions in liquid argon.[25] More recently, Conti *et al.*[26] applied the same method to improve the energy measurement of relativistic electrons in a liquid xenon detector using a single UV PMT to detect the scintillation signal. For 570 keV γ rays from ^{207}Bi, an energy resolution of $3\%(\sigma)$ was measured at 4 kV/cm by combining the charge and light signals. In our study, the improved light collection efficiency with two PMTs immersed in the liquid gives even better results.

Figure 5 shows the strong anticorrelation of charge and light signals measured with our detector for 662 keV γ rays from ^{137}Cs at 1 kV/cm. The energy resolution inferred from the light and charge signals separately is $10.3\%(\sigma)$ and $4.8\%(\sigma)$, respectively. The resolution from the charge signal is consistent with previously measured values.[7,24] The charge-light correlation angle θ, also shown in Fig. 5, is defined as the angle between the major axis of the charge-light ellipse and the X axis for light. θ can be roughly calculated as $\tan^{-1}(R_q/R_s)$, where R_s and R_q are the energy resolutions of the 662 keV peak from scintillation and ionization spectra, respectively. θ can also be found by a two-dimensional Gaussian fit to the charge-light ellipse of the 662 keV peak. A better energy resolution can be achieved by combining the charge and light signals as (see the Appendix on how to derive this equation),

$$\varepsilon_c = \frac{\sin\theta\varepsilon_s + \cos\theta\varepsilon_q}{\sin\theta + \cos\theta}, \tag{4}$$

where ε_c is the combined signal, in units of keV. ε_s and ε_q are scintillation light and charge based energies in units of keV. The charge-light combined energy resolution of 662 keV line is significantly improved to $1.7\%(\sigma)$.

The energy resolution from the charge-light combined spectrum, R_c, can be derived from Eq. (4) as,[27]

$$R_c^2 = \frac{\sin^2\theta R_s^2 + \cos^2\theta R_q^2 + 2\sin\theta\cos\theta R_{sq}}{(\sin\theta + \cos\theta)^2}, \tag{5}$$

where R_s and R_q are the energy resolutions from scintillation and ionization spectra, respectively. The covariance R_{sq} is the contribution from the correlation of the two signals. The magnitude of R_{sq} indicates the strength of anticorrelation (or correlation) between the scintillation and ionization signals. It is usually expressed in terms of correlation coefficient ρ_{sq},

$$\rho_{sq} = R_{sq}/(R_s R_q). \tag{6}$$

A value of ρ_{sq} close to -1 (1) indicates a very strong anticorrelation (correlation) of scintillation and ionization signals, while a zero ρ_{sq} means no correlation. In Eq. (5), R_s and R_q can be expressed as

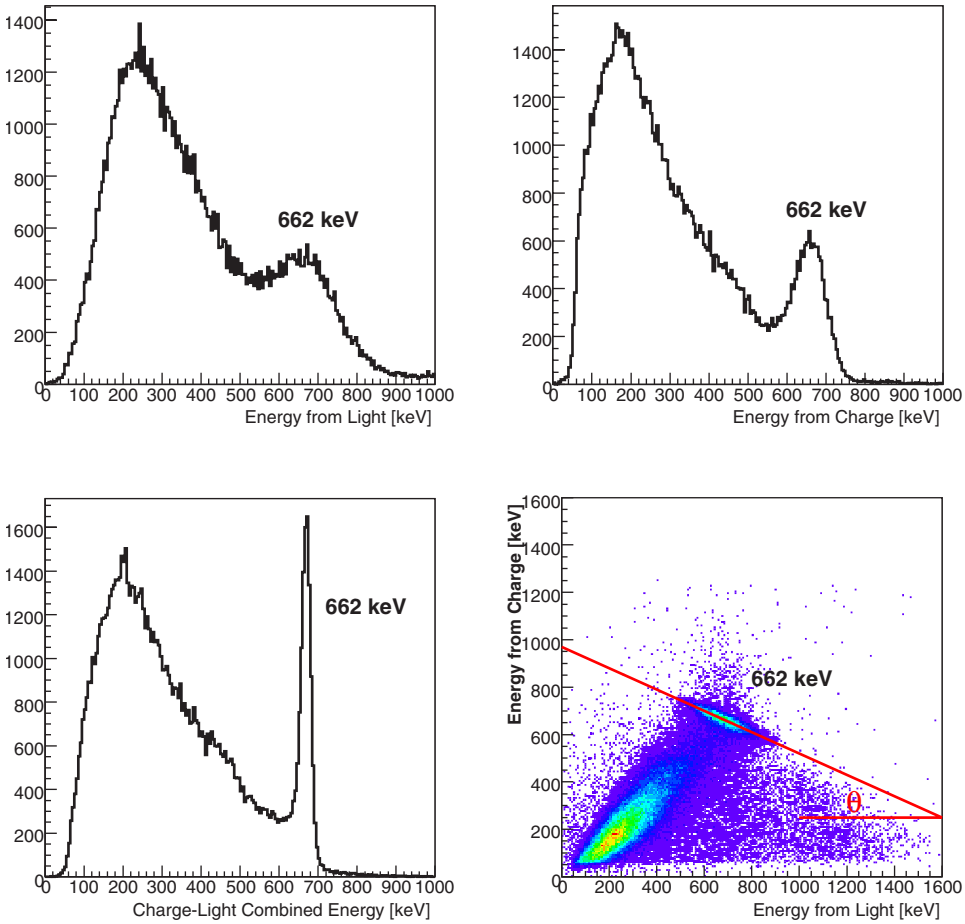

FIG. 5. (Color online) Energy spectra of ^{137}Cs 662 keV γ rays at 1 kV/cm drift field in liquid xenon. The top two plots are from scintillation and ionization, respectively. The strong charge-light anticorrelation is shown in the bottom-right plot. The straight line indicates the charge-light correlation angle. A charge-light combined spectrum (bottom-left) shows a much improved energy resolution of 1.7% (σ).

$$R_s^2 = R_{si}^2 + R_{sg}^2 + R_{ss}^2 \approx R_{si}^2 + R_{ss}^2, \tag{7}$$

$$R_q^2 \approx R_{qi}^2 + R_{qe}^2, \tag{8}$$

where R_{si} and R_{qi} are the energy resolution of scintillation and ionization, respectively, contributed by liquid xenon itself. They include the liquid xenon intrinsic resolution and the contribution from fluctuations of electron-ion recombination. R_{sg} is from the geometrical fluctuation of light collection. It is negligible in our result, since only events in the center of the detector were selected for the analysis. R_{ss} is from the statistical fluctuation of the number of photoelectrons N_{pe} in the PMTs. R_{ss} can be calculated roughly as $R_s = \sqrt{\left[1+\left(\frac{\sigma_g}{g}\right)^2\right]/N_{pe}}$, which includes the statistical fluctuations of the number of photoelectrons and the PMTs gain variation ($\sigma_g/g \sim 0.67$, based on the single-photoelectron spectrum). R_{qe} is from the equivalent noise charge (ENC) of the charge readout. ENC was measured to be between 600 and 800 electrons, depending on the drift field, from a test pulse distribution. R_{qe}=ENC/N_e, where N_e is the number of collected charges from the 662 keV peak. We note that we have neglected other contributions to the resolution of the charge measurement, such as from shielding grid inefficiency or pulse rise time variation, as they are subdominant compared to the electronic noise contribution.

Table I lists the energy resolution of the 662 keV γ-ray peak inferred from ionization, scintillation, and charge-light combined spectra at different drift fields. The quoted errors are statistical only. The correlation angle and the correlation

TABLE I. *Measured* energy resolutions (σ) and correlation coefficients for 662 keV gamma rays at different electric field values.

Field (kV/cm)	R_s (%)	R_q (%)	R_c (%)	θ (deg)	ρ_{sq}
0	7.9±0.3				
1	10.3±0.4	4.8±0.1	1.7±0.1	24.8	−0.87
2	10.5±0.3	4.0±0.1	1.8±0.1	20.8	−0.80
3	10.0±0.3	3.6±0.1	1.9±0.1	19.7	−0.74
4	9.8±0.3	3.4±0.1	1.8±0.1	19.1	−0.74

TABLE II. *Predicted* achievable energy resolutions in liquid xenon for light (R_{si}), charge (R_{qi}), and combined (R_{ci}) measurements, and charge-light correlation coefficient by removing instrumental noise contributions.

Field (kV/cm)	R_{si} (%)	R_{qi} (%)	R_{ce} (%)	R_{ci} (%)	ρ_{sqi}
0	6.0±0.3				
1	9.9±0.4	4.3±0.1	1.6±0.1	<1.0	−1.00
2	10.1±0.3	3.5±0.1	1.7±0.2	<1.2	−0.98
3	9.5±0.3	3.0±0.1	1.8±0.2	<1.2	−0.98
4	9.3±0.3	2.8±0.1	1.8±0.2	<1.0	−1.00

coefficient at each field are also presented. The energy resolution improves with increasing field for both scintillation and ionization, while the charge-light combined energy resolution is about the same at different fields. The best value achieved in this study is 1.7% (σ) at 1 kV/cm drift field. We should mention that during this work, we observed improvement of the energy resolution from both light and combined energy spectra when we used Teflon to enhance light collection,[16,29] while the energy resolution from the charge spectrum did not change.

The different value of the charge-light correlation coefficient at different fields indicates a more fundamental correlation coefficient between ionization and scintillation in liquid xenon. In fact, the energy resolution R_c from charge-light combined signals comes from two factors: One is the liquid xenon intrinsic energy resolution R_{ci}; another factor, R_{ce}, is contributed by external sources, such as the fluctuation of light collection efficiency on the light signal and fluctuation of electronic noise on the charge signal. The charge-light combined energy resolution can be written as follows:

$$R_c^2 = R_{ci}^2 + R_{ce}^2, \tag{9}$$

$$R_{ci}^2 = \frac{\sin^2\theta R_{si}^2 + \cos^2\theta R_{qi}^2 + 2\sin\theta\cos\theta R_{sqi}}{(\sin\theta + \cos\theta)^2}, \tag{10}$$

$$R_{ce}^2 \approx \frac{\sin^2\theta R_{ss}^2 + \cos^2\theta R_{qe}^2}{(\sin\theta + \cos\theta)^2}. \tag{11}$$

In these equations, R_{si} and R_{qi} are the liquid xenon energy resolution from scintillation and ionization, respectively, as previously discussed. R_{sqi} indicates the correlation between ionization and scintillation signals in liquid xenon. We can define the *intrinsic* correlation coefficient, ρ_{sqi}, of liquid xenon scintillation and ionization, similar to Eq. (6) for the *measured* charge-light correlation coefficient, but without instrumental noise contributions:

$$\rho_{sqi} = R_{sqi}/(R_{si}R_{qi}). \tag{12}$$

The energy resolution for scintillation R_{si} and ionization R_{qi} can be calculated based on Eqs. (7) and (8), from the measured values of correlation angle θ, statistical fluctuation of light detection R_{ss} and electronic noise contribution R_{qe}. The calculated values are listed in Table II. Table II also shows the intrinsic and external contributions, R_{ci} and R_{ce}, to the charge-light combined energy resolution. The values of R_{ci} and R_{ce} are calculated from Eqs. (9)–(11). The intrinsic correlation coefficients from Eq. (12) are also shown.

The intrinsic energy resolution in liquid xenon from the combined scintillation and ionization signals is estimated to be less than 1%. Only upper limits are given here since the uncertainties become large at such small values. The intrinsic correlation coefficients are closer to −1 than those measured from the experimental data including instrumental noisecontributions. This indicates near-perfect anticorrelation between ionization and scintillation in liquid xenon. We therefore expect that further improvement in the combined signal energy resolution can be achieved by increasing light collection efficiency and by minimizing electronic noise.

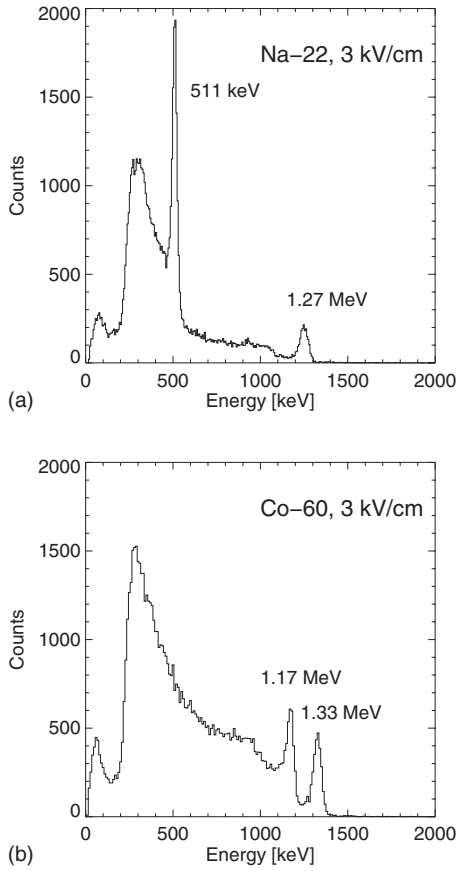

FIG. 6. Energy spectra of ^{22}Na and ^{60}Co γ-ray sources at 3 kV/cm, by combining charge and light signals.

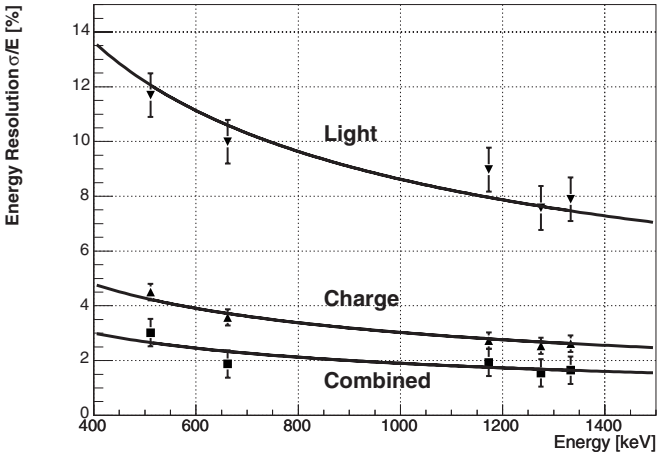

FIG. 7. Energy dependence of resolution measured from ^{22}Na, ^{137}Cs, and ^{60}Co at 3 kV/cm drift field.

C. Energy dependence of resolution

The improvement of the energy resolution by combining scintillation and ionization signals was studied at 3 kV/cm drift field as a function of γ-ray energy, using radioactive sources such as ^{22}Na (511 keV and 1.28 MeV), ^{137}Cs (662 keV), and ^{60}Co (1.17 and 1.33 MeV) (Fig. 6). The energy resolution from charge, light, and charge-light combined spectra is shown in Fig. 7. The data were fitted with an empirical function, $\sigma/E=\alpha/\sqrt{(E/\mathrm{MeV})}$, yielding for the parameter α (8.6±0.4)%, (3.0±0.4)%, and (1.9±0.4)% for light, charge, and combined spectra, respectively.

IV. CONCLUSION

We have shown that the energy resolution of MeV γ rays in liquid xenon can be significantly improved by combining simultaneously measured scintillation and ionization signals. The best resolution achieved is 1.7% (σ) for 662 keV γ rays at 1 kV/cm. This value is much better than that measured from scintillation [10.3% (σ)] or from ionization, [4.8% (σ)], separately. By summing the two signals, which are strongly anticorrelated, recombination fluctuations are reduced, resulting in improved energy resolution. At present, the energy resolution of the combined signal is still limited by external factors, such as light collection efficiency, PMT quantum efficiency, and charge readout electronic noise. By reducing the contribution from these factors, we estimate that the intrinsic energy resolution of MeV gamma rays in liquid xenon from charge-light combined signal should be less than 1%. The simultaneous detection of ionization and scintillation signals in liquid xenon, therefore, provides a practical way to improve the energy measurement with a resolution better than the Poisson limit, and possibly closer to the Fano limit.[10] On the other hand, the limit to the energy resolution of LXe might well be not determined by Fano statistics but rather connected to the liquid phase, for instance, to microscopic density nonuniformities of the liquid itself. It has been shown by Bolotnikov and Ramsey[28] that the energy resolution deteriorates as the density of Xe gas increases. The behavior was attributed to the formation of molecular clusters in high pressure and liquid xenon, but a more quantitative explanation is needed. Despite the limitation of energy resolution, the liquid phase offers far too many advantages for high energy radiation detection. The development of a LXeTPC which combines millimeter spatial resolution with 1% or better energy resolution, within a large homogeneous volume, is very promising for particle physics and astrophysics experiments.

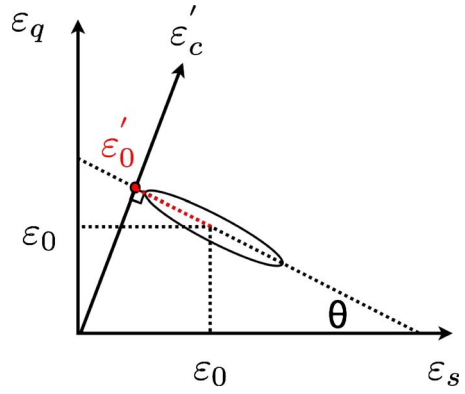

FIG. 8. (Color online) Illustration of how to combine charge ε_q and light ε_s into a combined signal ε'_c.

ACKNOWLEDGMENTS

This work was supported by a grant from the National Science Foundation (Grant No. PHY-02-01740) to the Columbia Astrophysics Laboratory. The authors would like to express their thanks to Tadayoshi Doke and Akira Hitachi for valuable discussions.

APPENDIX: DERIVATION OF THE EQUATION FOR THE COMBINED SIGNAL

Figure 8 illustrates how the charge and light signals are combined [Eq. (4)]. ε_q and ε_s are charge and light signals in units of energy (keV). ε_0 is the mean for both charge and light signals (e.g., ε_0=662 keV). θ is the charge-light correlation angle. By projecting the data points on the ellipse along the charge-light correlation line, we get a combined signal,

$$\varepsilon'_c = \sin\theta\varepsilon_s + \cos\theta\varepsilon_q. \tag{A1}$$

The mean of the combined signal is

$$\varepsilon'_0 = \sin\theta\varepsilon_0 + \cos\theta\varepsilon_0. \tag{A2}$$

We then normalize the combined signal in units of energy (keV) [Eq. (4)],

$$\varepsilon_c = \varepsilon'_c\frac{\varepsilon_0}{\varepsilon'_0} = \frac{\sin\theta\varepsilon_s + \cos\theta\varepsilon_q}{\sin\theta + \cos\theta}. \tag{A3}$$

*Present address: Department of Physics and Astronomy, University of Sheffield, UK.
†Present address: Physics Department, Yale University, New Haven, CT 06511.

[1] M. Danilov *et al.*, Phys. Lett. B **480**, 12 (2000).
[2] XENON Collaboration, E. Aprile *et al.*, Proceedings of the International Workshop on Techniques and Applications of Xenon Detectors (Xenon01), ICRR, University of Tokyo, Kashiwa, Japan, 2001 (World Scientific, Singapore, 2002), p. 165.
[3] G. J. Alner *et al.*, arXiv:astro-ph/0701858 (unpublished).
[4] D. Y. Akimov *et al.*, Astropart. Phys. **27**, 46 (2007).
[5] M. Yamashita *et al.*, Proceedings of the International Workshop on Techniques and Applications of Xenon Detectors (Xenon01), ICRR, University of Tokyo, Kashiwa, Japan, 2001 (World Scientific, Singapore, 2002), p. 136.
[6] MEG Collaboration, Paul Scherrer Institute, report, 1999 (unpublished).
[7] E. Aprile, A. Curioni, V. Egorov, K. L. Giboni, U. Oberlack, S. Ventura, T. Doke, K. Takizawa, E. L. Chupp, and P. P. Dunphy, Nucl. Instrum. Methods Phys. Res. A **461**, 256 (2001).
[8] V. Chepel, M. I. Lopes, A. Kuchenkov, R. Ferreira Marques, and A. J. P. L. Policarpo, Nucl. Instrum. Methods Phys. Res. A **392**, 427 (1997).
[9] T. Doke, J. Kikuchi, and F. Nishikido, Nucl. Instrum. Methods Phys. Res. A **569**, 863 (2006).
[10] U. Fano, Phys. Rev. **70**, 44 (1946); **72**, 26 (1947).
[11] T. Takahashi, S. Konno, T. Hamada, M. Miyajima, S. Kubota, A. Nakamoto, A. Hitachi, E. Shibamura, and T. Doke, Phys. Rev. A **12**, 1771 (1975).
[12] J. Jortner, L. Meyer, S. A. Rice, and E. G. Wilson, J. Chem. Phys. **42**, 4250 (1965).
[13] S. Kubota, A. Nakamoto, T. Takahashi, T. Hamada, E. Shibamura, M. Miyajima, K. Masuda, and T. Doke, Phys. Rev. B **17**, 2762 (1978).
[14] H. Ichinose, T. Doke, A. Hitachi, J. Kikuchi, K. Masuda, and E. Shibamura, Nucl. Instrum. Methods Phys. Res. A **322**, 216 (1992).
[15] J. Séguinot, G. Passardi, J. Tischhauser, and T. Ypsilantis, Nucl. Instrum. Methods Phys. Res. A **323**, 583 (1992).
[16] E. Aprile, A. Curioni, K.-L. Giboni, M. Kobayashi, K. Ni, and U. G. Oberlack, IEEE Trans. Nucl. Sci. **50**, 1303 (2003).
[17] XENON Collaboration, E. Aprile *et al.*, New Astron. Rev. **49**, 289 (2005).
[18] K. Ni, E. Aprile, D. Day, K. L. Giboni, J. A. M. Lopes, P. Majewski, and M. Yamashita, Nucl. Instrum. Methods Phys. Res. A **551**, 356 (2005).
[19] E. Aprile, P. Cushman, K. Ni, and P. Shagin, Nucl. Instrum. Methods Phys. Res. A **556**, 215 (2006).
[20] M. Yamashita, T. Doke, K. Kawasaki, J. Kikuchi, and S. Suzuki, Nucl. Instrum. Methods Phys. Res. A **535**, 692 (2004).
[21] E. Aprile, A. Bolotnikov, D. Chen, R. Muhkerjee, and F. Xu, Nucl. Instrum. Methods Phys. Res. A **480**, 636 (2002).
[22] T. Doke, A. Hitachi, J. Kikuchi, K. Masuda, H. Okada, and E. Shibamura, Jpn. J. Appl. Phys., Part 1 **41**, 1538 (2002).
[23] M. Miyajima, T. Takahashi, S. Konno, T. Hamada, S. Kubota, H. Shibamura, and T. Doke, Phys. Rev. A **9**, 1438 (1974).
[24] A. Curioni, E. Aprile, T. Doke, K. L. Giboni, M. Kobayashi, and U. G. Oberlack, Nucl. Instrum. Methods Phys. Res. A **576**, 350 (2007).
[25] H. J. Crawford, T. Doke, A. Hitachi, J. Kikuchi, P. J. Lindstrom, K. Masuda, S. Nagamiya, and E. Shibamura, Nucl. Instrum. Methods Phys. Res. A **256**, 47 (1987).
[26] EXO Collaboration, E. Conti *et al.*, Phys. Rev. B **68**, 054201 (2003).
[27] P. R. Bevington and D. K. Robinson, Am. J. Phys. **61**, 766 (1993).
[28] A. Bolotnikov and B. Ramsey, Nucl. Instrum. Methods Phys. Res. A **428**, 391 (1999).
[29] K. Ni, E. Aprile, K. L. Giboni, P. Majewski, and M. Yamashita, J. Instrum. **1**, P09004 (2006).